

Synthesis of Highly Fluorescent Copper Nanoclusters: Box-Behnken Design Based Statistical Modeling and Optimization

H. Sabzalipoor, E. Karimi and M. Nikkhah*

Department of Nanobiotechnology, Faculty of Biological Sciences, Tarbiat Modares University, Tehran, Iran

(Received 13 February 2022, Accepted 19 February 2022)

ABSTRACT

Copper nanoclusters (CuNCs) due to their fascinating physical and chemical properties and unique fluorescence characteristics have attracted great attention in the past decade. Compared to gold and silver NCs, CuNCs are relatively cheaper which makes them more attractive in development of sensing platforms. However, they still have limitations such as low quantum yield and susceptibility to oxidation. Herein, BSA as a scaffold, stabilizer, and protective agent has been used for CuNCs synthesis via a bottom-up approach. The effects of synthesis time, copper salt and BSA concentration in fluorescence intensities of the NCs were studied, modeled, and optimized in the form of Box-Behnken design. Finally, to validate the model, CuNCs were synthesized by the predicted optimal conditions and their optical properties were compared with the model predictions. The BSA/CuNCs synthesized in this work showed two fluorescence peaks at 400 nm and 670 nm relating to NCs with different sizes. The model proposed the optimal conditions for synthesis of 400 nm emitting CuNCs as copper salt concentration of 10.05 mM, BSA concentration of 27.69 mg ml⁻¹ and synthesis time of 3.3 h. The optimal condition for production of 670 nm emitting CuNCs was determined as copper salt concentration of 19.97 mM, BSA concentration of 10.1 mg ml⁻¹ and synthesis time of 3.61 h. CuNCs were then synthesized for validation of the model, and their emission at 400 nm and 670 nm were 90.6% and 94.9% in agreement with the model predictions, respectively.

Keywords: Copper nanocluster, BSA, Fluorescence, Box-Behnken, Optimization

INTRODUCTION

In the past decades, there has been extensive researches on plasmonic nanoparticles due to their unique properties which are dependent on their size and shape and, interestingly, often being different from their bulk counterparts. As the particle further becomes smaller approaching the electrons Fermi wavelength which is 5 Å for Ag and Au [1] and 4.5 Å for Cu [2], the continuous density of states turns into discrete levels of energy resulting into remarkable different electrical, chemical, and optical properties in comparison to nanoparticles. Considering this regime of size, metal nanoclusters resemble molecules and show a strong size-dependent fluorescence emission upon excitation [3].

In the past decades protein conjugated fluorescent gold nanoclusters have been attracted a lot of attention in sensing

and biosensing researches due to their excellent photostability. However, fewer studies have devoted their concentration on the fluorescent copper nanoclusters (CuNCs) which are showing almost the same optical properties as their silver and gold counterparts. CuNCs are cost effective, have great fluorescent properties, and show good solubility in water. They have emerged as novel nanomaterials with fascinating photoluminescent and catalytic activity, and attracted growing interests in several different areas such as sensing [4], catalysis [5], and bio-labeling [6]. The synthesis of CuNCs is still facing limitations such as difficulties in size control, the oxidation susceptibility and irreversible aggregation [7]. The optical properties of CuNCs can be controlled by the size of the metal core, the physicochemical properties of the stabilizing agents and the synthesis parameters such as the concentration and the nature of reducing agents, reaction temperature, and reaction time. The use of chemical stabilizing agents or biological macromolecules like DNA

*Corresponding author. E-mail: m_nikkhah@modares.ac.ir

[8,9], proteins (papain) [10], BSA [11,12], trypsin [13] and egg white [14] has been reported to reduce fusion and aggregation of nanoclusters. CuNCs synthesized by BSA have been shown to be stable and compatible to a variety of chemical conditions and environments [15]. BSA is used as both reducing agent and stabilizer in the process of metal cluster synthesis. Cu^{2+} is reacted with the thiols in the BSA forming stable Cu-S bonds which leads into production of an inert layer of BSA on the surface of the CuNCs. BSA possesses 17 disulfide bonds as well as one free cysteine which have strong affinity for metal ions [16]. However, BSA is not considered as an efficient reducing agent and another chemical reducer is usually employed in the procedure.

In this paper, Box-Behnken design (BBD) and single factor experiments were used to optimize three major factors involving in synthesis of BSA stabilized CuNCs including copper salt concentration, BSA concentration and synthesis time. The experimental validation of optimized synthesis condition was performed.

MATERIAL AND METHODS

Chemicals and Reagents

BSA was obtained from Applichem (Germany). Copper(II) sulfate and sodium hydroxide were purchased from Merck. Hydrazine monohydrate was from Sigma-Aldrich.

Characterization Methods

UV-Vis and fluorescence measurements were performed by Cytation™ 3 (BioTek). Dynamic Light Scattering (DLS) data were obtained using Malvern zetasizer (nano zs). Transmission Electron Microscopy (TEM) images were taken by Carl Zeiss Auriga 60 cross-beam. All the data were analyzed using SPSS, Design Expert 11 and Microsoft Office Excel.

The Synthesis of Nanoclusters and Optimization Method

Three-level-three-factor BBD was employed for optimization of CuNCs fluorescence intensity in two different emission wavelengths of 400nm and 670 nm. Since BSA concentration (X1), copper salt concentration

(X2) and synthesis time (X3) were thought to have significant effects on fluorescence intensity, they were selected as the critical variables to be optimized to get the highest fluorescence intensity (Y). The synthesis of NCs was conducted with adding varying amount of BSA (10 to 30 mg), to 0.3 ml of CuSO_4 with varying concentration (5 to 20 mM), followed by stirring at room temperature for 10 min. Then, 40 μl of NaOH (1 M) was introduced to the solution to adjust the pH to 12. The mixture was subsequently injected by 50 μl of $\text{N}_2\text{H}_4 \cdot 2\text{H}_2\text{O}$ and stirred at room temperature for varying synthesis time (2 to 4 h). The ranges of the independent variables (X1, X2, and X3) were chosen based on preliminary single-factor-test. Then, 15 treatments were done based on the BBD experimental design, and high, middle, and low levels of the coded values were designated for the variables as -1, 0 and 1, respectively. The actual levels and the corresponding codes of the independent variables in the BBD experimental design matrix are shown in Table 1. Generally, in the process of BBD optimization the statistically designed experiments are performed to estimate the coefficients of the mathematical model, aiming to predict the responses and to verify the model [17]. The statistical software of Design Expert 11 (Stat-Ease Inc.) was utilized to perform all the BBD based experimental design, statistical analysis of variance (ANOVA), analysis of regression model, as well as to draw three-dimensional graphs of the response surface and the two-dimensional contour plots.

RESULTS AND DISCUSSIONS

The Results of Single-factor Experiments

Effect of BSA concentration on fluorescence properties of Cu-NCs. In this study, BSA was used to direct synthesis of CuNCs due to the stability it bestows to the NCs. Figure 1 shows the UV-Vis spectra of the CuNCs synthesized at different concentration of Cu^{2+} . By increasing the copper salt concentration, the absorption at 330 nm increased, which could imply the gradual formation of more and larger NCs in the solution. The synthesized CuNCs emitted at 400 nm and 670 nm, referred to as blue emitting and red emitting Cu-NCs, respectively (Fig. 2). The effects of three concentrations of BSA on fluorescence intensity and emission spectrum of CuNCs are depicted in Fig. 2. As

Table 1. The Box-Behnken Design and the Response Values for Fluorescence Intensities at 400 nm and 670 nm (Em400 and Em670, Respectively). All Three Factors were Considered at Three Levels Including BSA Concentrations of 10, 20 and 30 mg ml⁻¹, Copper salt Concentrations of 5, 12.5 and 20 mM, and Synthesis Time of 2, 3 and 4 h

Run	A: BSA concentration (mg ml ⁻¹)	B: copper salt concentration (mM)	C: Time	Em400	Em670
1	30	20	3	5154.2	212.1
2	30	5	3	6853.0	12.0
3	20	12.5	3	6399.0	320.0
4	20	5	4	4484.7	15.3
5	30	12.5	2	5789.5	34.0
6	20	12.5	3	7233.0	358.0
7	10	12.5	4	1968.5	1520.8
8	20	20	2	3429.5	1959.1
9	10	20	3	1704.0	3742.0
10	10	12.5	2	2189.6	2182.0
11	20	5	2	4576.5	7.1
12	30	12.5	4	8135.0	86.5
13	20	20	4	2657.3	2392.6
14	10	5	3	3557.0	2.0
15	20	12.5	3	7242.0	435.0

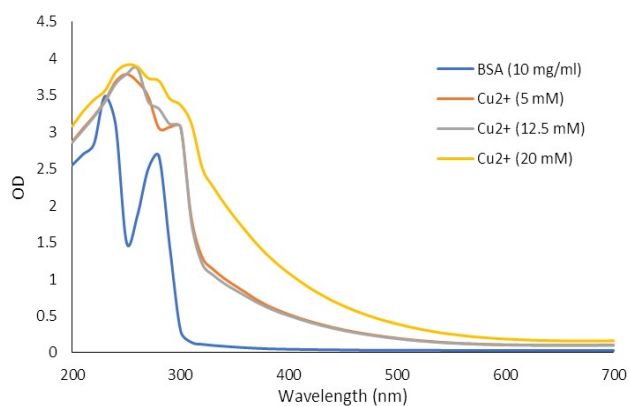


Fig. 1. Absorption spectra of CuNCs synthesized at three copper salt concentrations by BSA (10 mg ml⁻¹).

can be seen, when the concentration of Cu²⁺ was as low as 5 mM, only one peak was observed at 400 nm; its intensity was not significantly changed by increments in BSA

concentration (Fig. 2a). The effect of BSA concentration on CuNCs fluorescence intensity was the most prominent when copper salt concentration was 12.5 mM. In this concentration both 400 nm and 670 nm peaks were affected by increasing BSA concentration (Fig. 2b). At copper salt concentration of 20 mM, emission at 400 nm was weak and the intense emission at 670 nm was significantly affected by various concentration of BSA (Fig. 2c).

Effect of copper salt concentration on fluorescence properties of CuNCs. The effects of Cu²⁺ (5, 6, 8, 10, 12.5 and 20 mM) at BSA concentration of 20 mg ml⁻¹ and synthesis time of 3 h on the fluorescence properties of NCs were studied. As shown in Fig. 3a, the fluorescence intensity at 400 nm is inversely correlated with copper salt concentration, but the emission at 670 nm is proportional to the copper salt concentration. It can be suggested that by increasing the concentration of Cu²⁺ the smaller NCs which emit at 400 nm grow to larger NCs emitting at 670 nm.

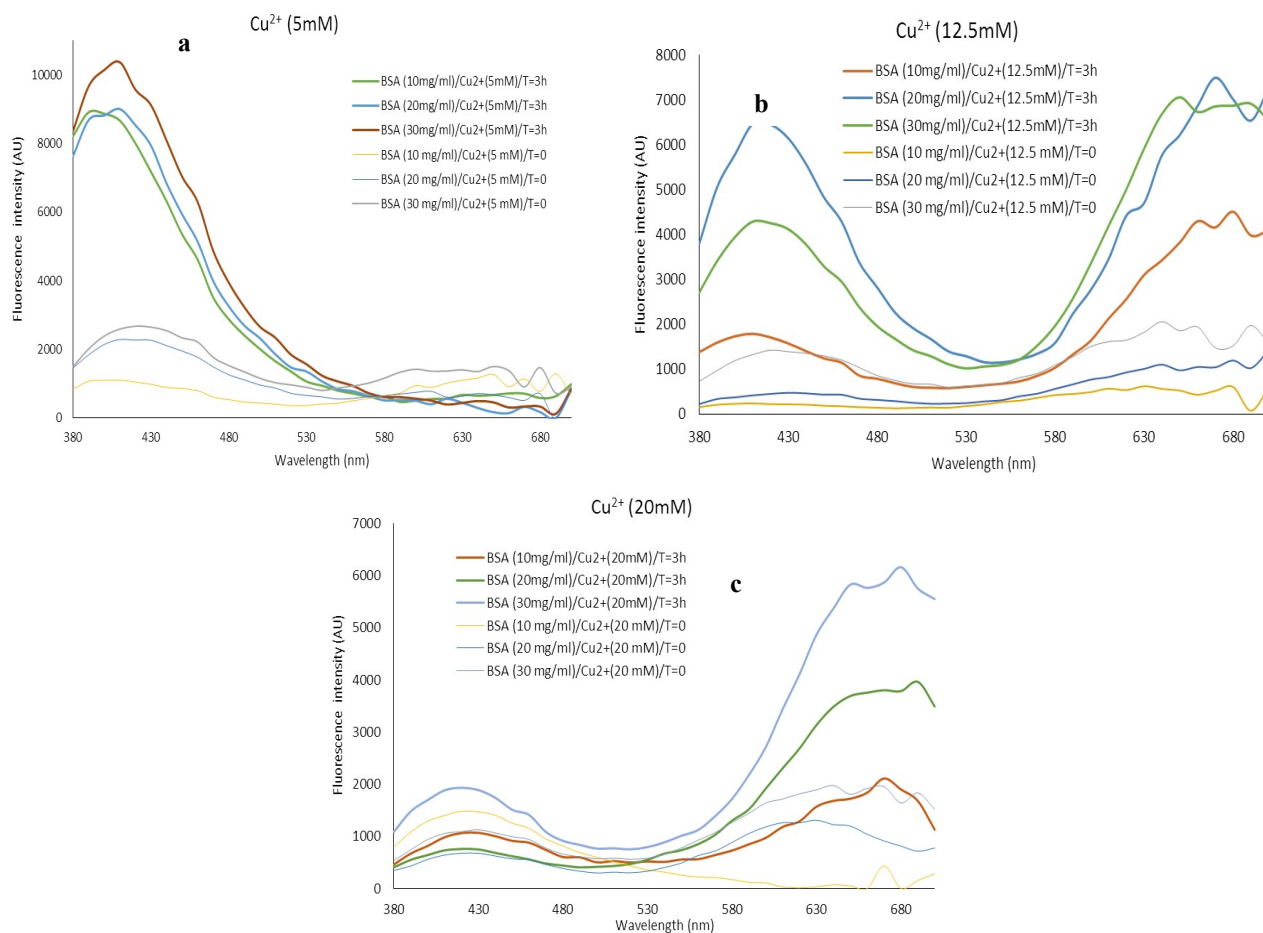


Fig. 2. The effect of three concentrations of BSA on emission spectra of CuNCs synthesized at three copper salt concentrations a) 5 mM, b) 12.5 mM, c) 20 mM and synthesis time of 3 h. Excitations were done at 350 nm).

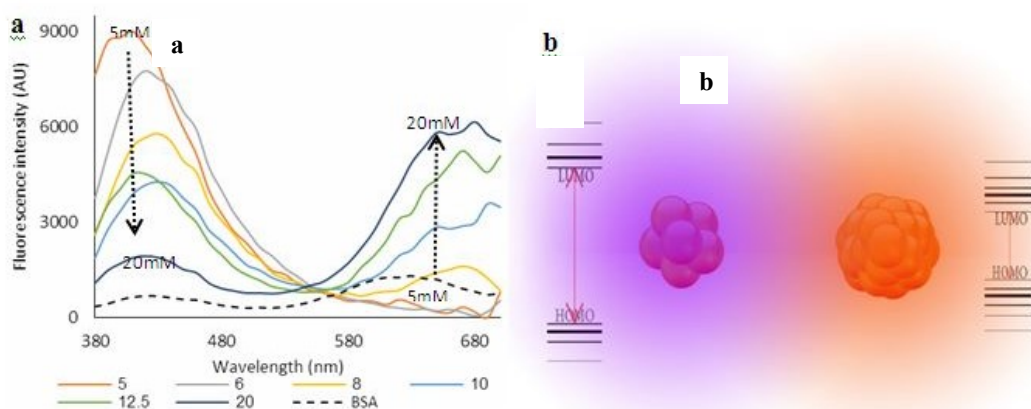


Fig. 1. a) The effect of copper salt (Cu^{2+}) concentration on fluorescence intensity and emission spectra of CuNCs synthesized by BSA (20 mg ml^{-1}) for 3 h. The intrinsic fluorescence intensity of BSA (20 mg ml^{-1}) is shown with black dashed line. b) Schematic representation of the effect of increasing copper concentration on the size of CuNCs and the bandgap between HOMO and LUMO.

When the number of atoms in a cluster increases, the gap between the highest occupied molecular orbital (HOMO) and the lowest unoccupied molecular orbital (LUMO) shrinks, leading into emission of photons at longer wavelengths [18]. At first, only tiny clusters with small number of atoms form in the solution. These have the widest gap between HOMO and LUMO which leads into emission of photons with the highest energy (Fig. 3b). Then, by increasing of Cu^{2+} concentration, larger clusters with smaller gap between HOMO and LUMO appear, resulting in emission at both 400 nm and 670 nm. By further increasing the Cu^{2+} concentration to 20 mM most of the small clusters have grown to larger ones which emit at 670 nm.

Further characterization of NCs was performed by TEM and DLS analysis (Fig. 4 and Table S1). As can be seen in Fig. 4a, at lower concentration of copper salt there was a group of BSA stabilized NCs with the dimension of about 5 nm. By increasing the copper salt concentration another group of BSA stabilized NCs with the average diameter of about 11 nm were observed (Figs. 4b and c). DLS measurements of the reaction at increasing amount of copper salt revealed that at lower concentrations of Cu^{2+} up to 8 mM, the particles with the size of around 5 nm existed. By increasing copper salt concentration, a second class of particles appeared with the sizes of around 11 nm. These two classes of nanoparticles could be attributed to two groups of BSA stabilized NCs that emit at 400 nm and 670 nm.

Effect of synthesis time on fluorescence behavior of CuNCs. The effect of synthesis time on fluorescence properties of CuNCs was investigated (Fig. 5). No significant difference in fluorescence intensity of CuNCs at both 400 nm and 670 nm was observed among synthesis times of 2, 3 and 4 h. The concentrations of BSA and copper salt were 20 mg ml^{-1} and 12.5 mM , respectively, in these experiments.

Optimization of Experiment Conditions by RSM

Box-Behnken designs are applied to produce higher order response surfaces using fewer required runs than a normal factorial designs. The Box-Behnken Design of the experiment is presented in Table 1. As can be seen, there was a considerable variation in the fluorescence intensity of

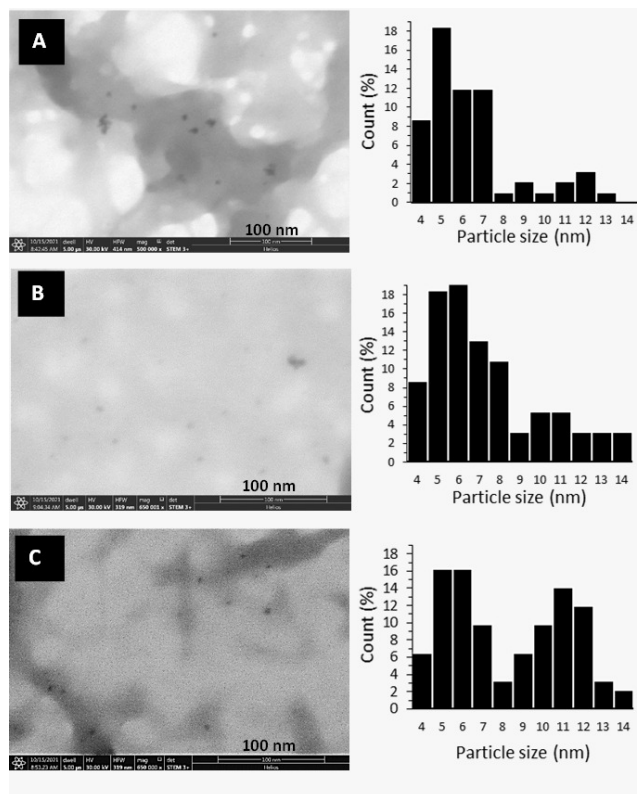


Fig. 4. TEM images and size distribution analysis of CuNCs synthesized at copper salt concentrations of 5 mM (A), 2.5 mM (B) and 20 mM (C) by BSA (20 mg ml^{-1}) for 3 h. Image analysis was done by Adobe CS4 on more than 70 random dots on each sample.

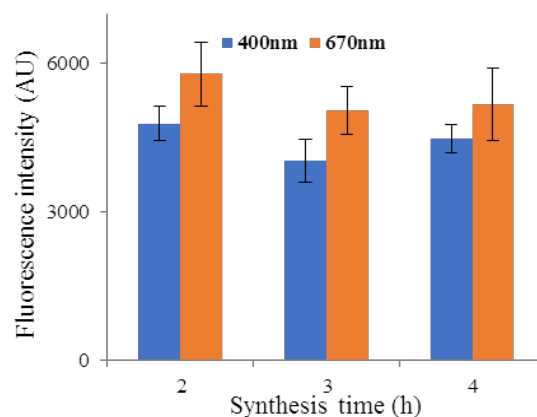


Fig. 5. The effect of different synthesis time of 2, 3 and 4 h on fluorescence intensity of CuNCs at 400 nm and 670 nm. The concentration of BSA and copper salt were 20 mg ml^{-1} and 12.5 mM , respectively.

CuNCs synthesized at different conditions. By using multiple regression analysis on independent and dependent variables, an equation can be obtained to predict fluorescence intensity at 400 nm and 670 nm.

Response 1: Fluorescence Intensity at 400 nm

The analysis of variance (ANOVA) conducted on the fluorescence intensities at 400 nm are shown in Table 2. The p-value of <0.007 and the associated F-value of 12.18 indicated that the presented regression model was significant. Also, the insignificance of F-value for lack of fit (3.27) implied that the model was valid. The R2 value (0.96) confirmed that there was a well correlation between the independent variables and the response. The p-values of coefficients of Eq. (1) are listed in Table 2. By having p-values less than 0.05, significant differences were observed with linear (A, B and C) and quadratic coefficient (A², B² and C²) while other terms are non-significant (Table 2).

$$FL_{400} = 6958 + (2064.08 * A) - (815.777 * B) + (157.534 * C) + (38.5309 * AB) + (641.647 * AC) - (170.076 * BC) - (953.669 * A^2) - (1687.3 * B^2) - (1483.7 * C^2)$$

A =BSA concentration (mg ml⁻¹)

B = Copper salt concentration (mM)

C = Time of synthesis (h)

(1)

The Eq. (1) can better graphically represented by the contour and three dimensional plots (Fig. 6). These plots depict the effect of each variable at all experimental levels on the response and the mutual interactions between the variables. Figure 6 shows the relationships between the fluorescence intensity at 400 nm and BSA concentration, copper salt concentration and time of CuNCs synthesis. In the contour and response surface plots, fluorescence intensity at 400 nm was plotted along with two variables being continuous, while the third one remained steady at its center value of the testing range (zero level). It can be seen that minor alteration in some of the variables could significantly affects the fluorescence intensity of NCs at 400 nm. These plots show that the NCs fluorescence intensity can be affected mostly by BSA concentration. The effect of copper salt concentration on the fluorescence intensity at 400 nm was also significant but was less than the effect of BSA concentration. As can be seen, increasing the concentration of Cu²⁺ led to the enhancement of fluorescent intensity at first, but not all the way. When the copper salt concentration passes 12.5 mM, the fluorescence intensity gradually decreases, which can be due to the quenching of NCs by the excess amount of Cu²⁺ in the reaction [19]. The synthesis time does not significantly influence the response. Considering the slopes in contour and 3D plots (Fig. 6) and also the significance of the regression coefficients of the quadratic polynomial model (Table 2), it

Table 2. The ANOVA of Fluorescence Intensities of NCs at 400 nm

Source	Sum of squares	df	Mean square	F-value	p-value	
Model	6.067E+07	9	6.741E+06	12.18	0.0066	Significant
A-BSA concentration	3.408E+07	1	3.408E+07	61.59	0.0005	
B-Copper salt concentration	5.324E+06	1	5.324E+06	9.62	0.0268	
C-Time	1.985E+05	1	1.985E+05	0.3588	0.5753	
AB	5938.52	1	5938.52	0.0107	0.9215	
AC	1.647E+06	1	1.647E+06	2.98	0.1451	
BC	1.157E+05	1	1.157E+05	0.2091	0.6667	
A ²	3.358E+06	1	3.358E+06	6.07	0.0570	
B ²	1.051E+07	1	1.051E+07	19.00	0.0073	
C ²	8.128E+06	1	8.128E+06	14.69	0.0122	
Residual	2.767E+06	5	5.534E+05			
Lack of fit	2.298E+06	3	7.661E+05	3.27	0.2430	Non significant
Pure error	4.688E+05	2	2.344E+05			
Cor total	6.344E+07	14				

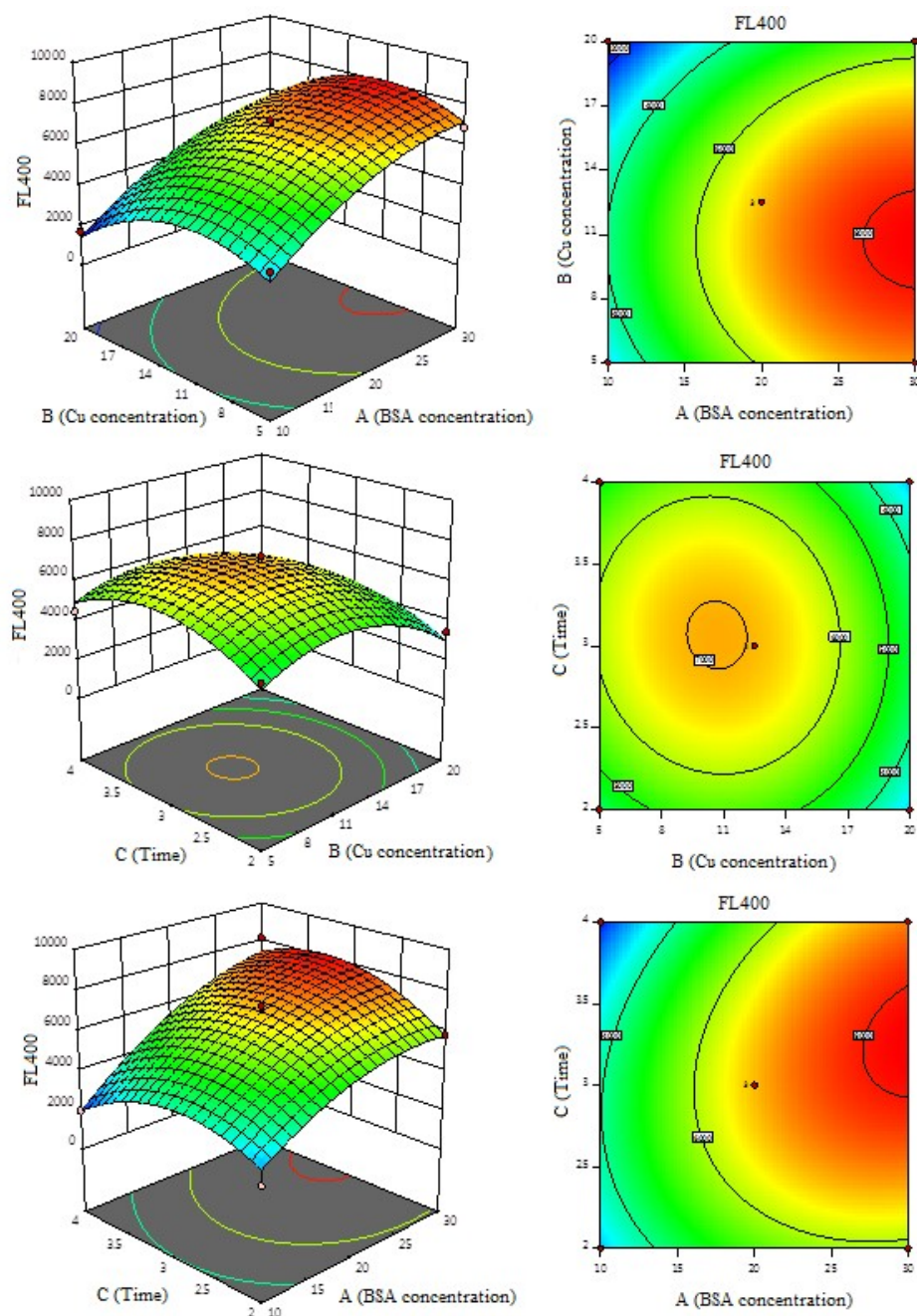


Fig. 6. Three-dimensional response surface (left) and contour plots (right) showing the effect of the BSA concentration (A), copper salt concentration (B) and time (C) and their mutual interactions on the fluorescence intensity of CuNCs at 400 nm.

can be concluded that BSA concentration is the most significant variable affecting fluorescence intensity at 400 nm followed by copper salt concentration and synthesis time.

Response 2: Fluorescence Intensity at 670 nm

As mentioned earlier, statistical models can help us to identify the impact of each factor and their mutual interactions on the response. The results of ANOVA

conducted on the fluorescence intensities at 670 nm are shown in Table 3. The fitness quality of the proposed model can statistically be judged by the coefficient of determination. Here in, this value was determined as $R^2 = 0.9915$ implying that there was a perfect correlation between the experimental data and the empirical model. The data presented in Table 3 (p-value of 0.0001 and F-value of 64.94) indicated that the model was highly significant. The data variation around the model can be found out by using the lack of fit (LOF) parameter. If there is a well fitness between the data and the model, LOF would not be significant.

This model ($R^2 > 0.99$) indicated that the role of BSA and copper salt concentration were highly significant. The fluorescence intensity at 670 nm was conversely related to BSA concentration. However, the effect of copper salt concentration on the response was much more prominent. The model demonstrated that the fluorescence intensity at 670 nm was significantly enhanced when copper salt concentration was increased. It can be concluded that the fluorescence intensity of NCs at 670 nm is proportional to the amount of BSA in the reaction and is inversely related to copper salt concentration. The interaction between these three factors and their influence on the fluorescence intensity at 670 nm is presented by Eq. (2); and graphically represented by the contour and three dimensional plots (Fig. 7).

$$\begin{aligned}
 FL670 = & 371 - (887.781 * A) + (1033.67 * B) - (20.8786 * \\
 & C) - (884.975 * AB) + (178.431 * AC) + (106.335 * BC) + \\
 & (241.644 * A^2) + (379.38 * B^2) + (343.169 * C^2) \\
 A = & \text{BSA concentration (mg ml}^{-1}\text{)} \\
 B = & \text{Copper salt concentration (mM)} \\
 C = & \text{Time of synthesis (h)}
 \end{aligned}
 \tag{2}$$

Verification of the Predictive Models

Optimum predicted conditions for CuNCs synthesis to get the maximum fluorescence intensity were empirically tested (Table 4). The results showed that the model has accuracy of more than 90% in predicting the experimental results.

Stability of Cu-NCs

The stability of CuNCs is considered as an important feature which plays a key role in their application in biosensing platforms. The use of CuNCs has been reported to be challenging as their stability in aqueous solution is fairly low [20,21]. Here in, the fluorescence stability of CuNCs was followed for up to one month. As can be seen in Fig. 8, results showed that NCs optimized to have maximum fluorescence intensity at 400 nm emission lost more than 20% of their fluorescence intensity after 4 days, but since then they remained highly fluorescent by emitting 73% of their max illumination after 30 days from the synthesis. On

Table 3. The ANOVA of Fluorescence Intensity Results at 670 nm

Source	Sum of squares	df	Mean square	F-value	p-value	
Model	1.919E+07	9	2.133E+06	64.94	0.0001	Significant
A-BSA concentration	6.305E+06	1	6.305E+06	192.00	< 0.0001	
B-Copper salt concentration	8.548E+06	1	8.548E+06	260.29	< 0.0001	
C-Time (Cu-NC synthesis)	3487.32	1	3487.32	0.1062	0.7577	
AB	3.133E+06	1	3.133E+06	95.39	0.0002	
AC	1.274E+05	1	1.274E+05	3.88	0.1060	
BC	45228.45	1	45228.45	1.38	0.2934	
A ²	2.156E+05	1	2.156E+05	6.57	0.0505	
B ²	5.314E+05	1	5.314E+05	16.18	0.0101	
C ²	4.348E+05	1	4.348E+05	13.24	0.0149	
Residual	1.642E+05	5	32839.74			
Lack of fit	1.573E+05	3	52444.23	15.28	0.0621	Non significant
Pure error	6866.00	2	3433.00			
Cor total	1.936E+07	14				

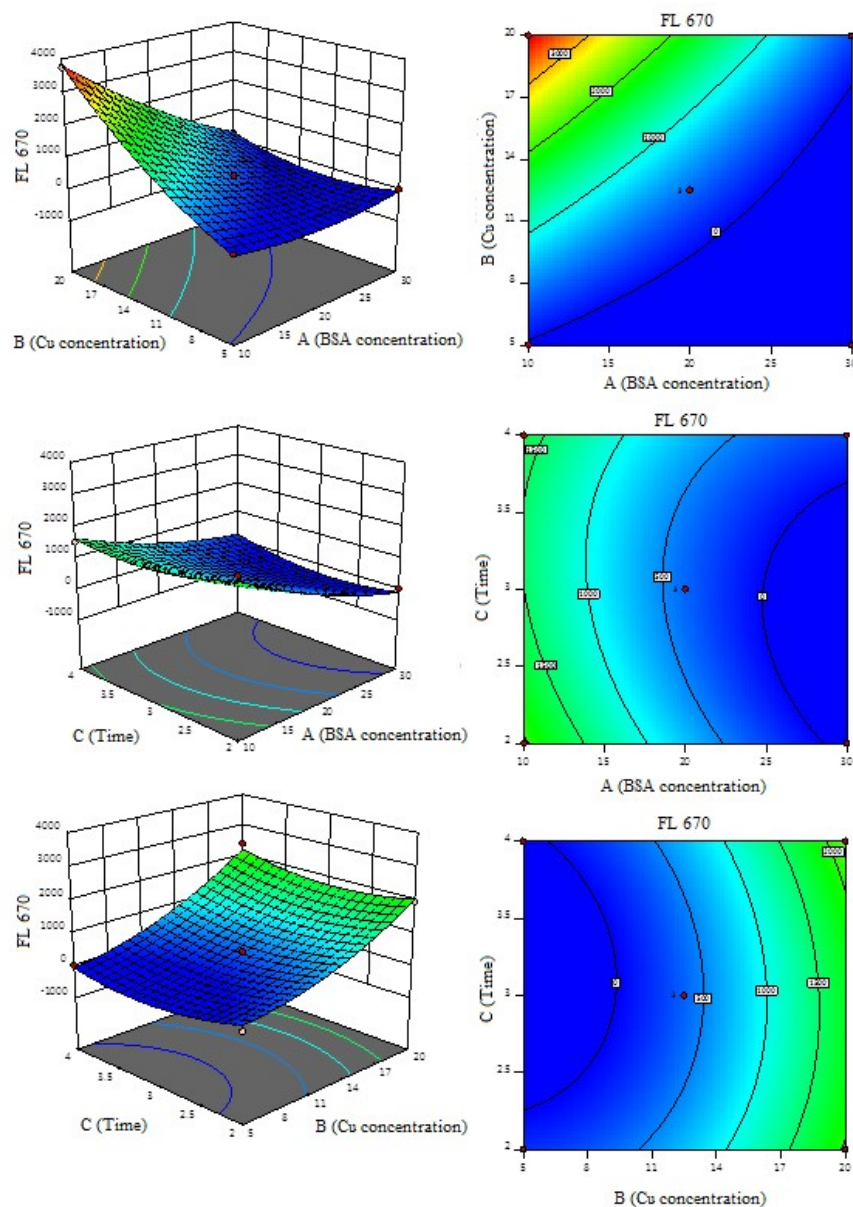


Fig. 7. Three-dimensional response surface (left) and counter plots (right) showing the effect of the BSA concentration (A), copper salt concentration (B) and time of CuNCs synthesis (C) on the fluorescence intensity at 670 nm.

Table 4. Comparison between the Predicted and Observed Fluorescence Intensities on CuNCs Synthesized at Optimal Conditions Predicted by the Model to have the Maximum Fluorescence Intensities at 400 nm and 670 nm

	BSA concentration (mg ml ⁻¹)	Copper salt concentration (mM)	Synthesis time (h)	Model Max FL prediction	Result	Accuracy
Em 400	27.69	10.05	3.30	7951	7263	90.6%
Em 670	10.1	19.97	3.61	3839	3644	94.9%

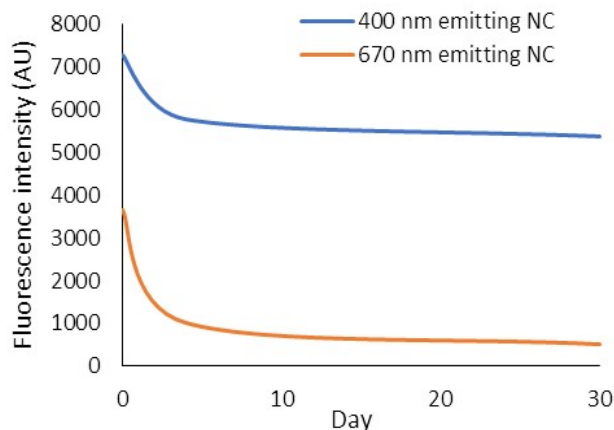


Fig. 8. Fluorescence stability of two optimized CuNCs at 4 °C.

the other hand, 670 nm emitting CuNCs have shown much less fluorescence stability and lost 70% and 85% of their emission intensity after 4 and 30 days respectively.

CONCLUSIONS

Aiming to discover the best synthesis conditions for CuNCs, we have used Box-Behnken design (BBD) and single factor experiments to optimize three major factors involving in the fluorescence intensity of CuNCs; these factors include copper salt concentration, BSA concentration and synthesis time.

It was found that the main factors involved in fluorescence intensity of 400 nm emitting NCs are the concentration of BSA and then, with the less impact, the concentration of copper salt. On the other hand, the fluorescence intensity of 670 nm emitting NCs is mainly governed by the copper salt concentration and then the BSA concentration. The models demonstrated in this study suggested that the synthesis time is not significantly effective on fluorescence intensity at 400 nm and 670 nm. The optimal conditions presented by the model for the synthesis of the best nanoclusters in terms of fluorescence intensity at 400 nm and 670 nm were experimentally tested showing validity of 90 and 94%, respectively.

Given the unique characteristics of CuNCs, such as biocompatibility, high fluorescence, low photo-bleaching as well as non-toxicity, this study can be a step forwards in

producing nanoclusters for a variety of applications.

ACKNOWLEDGEMENTS

We acknowledge the Research council of Tarbiat Modares for funding this research. Leibniz Institute of Age Research-Fritz Lipmann Institute (FLI) Jena is acknowledged for providing access to TEM and Katrin Buder (FLI) for her help with TEM imaging.

REFERENCES

- [1] C. Zhou, J. Yu, Y. Qin, J. Zheng, *Nanoscale* 4 (2012) 4228.
- [2] Y. Han, K.C. Lai, A. Lii-Rosales, M.C. Tringides, J.W. Evans, P.A. Thiel, *Surface Sci.* 685 (2019) 48.
- [3] H. Xu, K.S. Suslick, *Adv. Mater.* 22 (2010) 1078.
- [4] Y. An, Y. Ren, M. Bick, A. Dudek, E.H.-W. Waworuntu, J. Tang, J. Chen, B. Chang, *Biosensors and Bioelectronics* 154 (2020) 112078.
- [5] S. Han, R.A. Ciufu, B.R. Wygant, B.K. Keitz, C.B. Mullins, *ACS Catal.* 10 (2020) 4997.
- [6] E. Shokri, M. Hosseini, A.A. Sadeghan, A. Bahmani, N. Nasiri, S. Hosseinkhani, *Sensor Actuat. B-Chem.* 321 (2020) 128634.
- [7] M. Zhao, A.-Y. Chen, D. Huang, Y. Zhuo, Y.-Q. Chai, R. Yuan, *Anal. Chem.* 88 (2016) 11527.
- [8] A. Rotaru, S. Dutta, E. Jentsch, K. Gothelf, A. Mokhir, *Angew. Chem. Int. Edit.* 49 (2010) 5665.
- [9] G. Liu, Y. Shao, J. Peng, W. Dai, L. Liu, S. Xu, F. Wu, X. Wu, *Nanotechnology* 24 (2013) 345502.
- [10] H. Miao, D. Zhong, Z. Zhou, X. Yang, *Nanoscale* 7 (2015) 19066.
- [11] Y. Zhong, J. Zhu, Q. Wang, Y. He, Y. Ge, C. Song, *Microchimica Acta* 182 (2015) 909.
- [12] C. Wang, C. Wang, L. Xu, H. Cheng, Q. Lin, C. Zhang, *Nanoscale* 6 (2014) 1775.
- [13] W. Wang, F. Leng, L. Zhan, Y. Chang, X.X. Yang, J. Lan, C.Z. Huang, *Analyst* 139 (2014) 2990.
- [14] J.R. Bhamore, S. Jha, A.K. Mungara, R.K. Singhal, D. Sonkeshariya, S.K. Kailasa, *Biosens. Bioelectron.* 80 (2016) 243.
- [15] X. Yang, J. Wang, D. Su, Q. Xia, F. Chai, C. Wang, F. Qu, *Dalton T.* 43 (2014) 10057.

- [16] R.S. Aparna, A.D. JS, N. John, K. Abha, S.S. Syamchand, S. George, *Spectrochimica Acta Part A: Molecular and Biomolecular Spectroscopy* 199 (2018) 123.
- [17] D. Baş, I.H. Boyacı, *Journal of food engineering* 78 (2007) 836.
- [18] M. Pereiro, D. Baldomir, *arXiv preprint physics/0702238* (2007).
- [19] H. Wu, X. He, B. Yang, C. Li, L. Zhao, *Angew. Chem. Int. Edit.* 60 (2021) 1535.
- [20] L. Xiaoqing, L. Ruiyi, L. Zaijun, S. Xiulan, W. Zhouping, L. Junkang, *New J. Chem.* 39 (2015) 5240.
- [21] R.S. Aparna, J.S.A. Devi, R.R. Anjana, J. Nebu, S. George, *Analyst* 144 (2019) 1799.